ISSN 0036-0236, Russian Journal of Inorganic Chemistry, 2017, Vol. 62, No. 12, pp. 1619–1623. © Pleiades Publishing, Ltd., 2017.
Original Russian Text © N.M. Berezina, Vu Thi Thao, D.B. Berezin, M.I. Bazanov, 2017, published in Zhurnal Neorganicheskoi Khimii, 2017, Vol. 62, No. 12, pp. 1614–1619.

PHYSICAL METHODS OF INVESTIGATION

Synthesis and Redox Characteristics of Iron Complexes with Triphenylsubstituted Corrols in the Presence of Argon and Oxygen

N. M. Berezina*, Vu Thi Thao, D. B. Berezin, and M. I. Bazanov**

Ivanovo State University of Chemistry and Technology, Research Institute of Macroheterocycles, Ivanovo, 153000 Russia

**e-mail: sky_berezina@rambler.ru*

***e-mail: berezin@isuct.ru*

Received October 4, 2016

Abstract—*para*-Substituted iron *meso*-triphenylcorrole derivatives [Fe(*ms*-*p*-R-Ph)$_3$Cor] containing electron-donating (R = OMe) and electron-drawing (R = NO_2) groups in phenyl rings are synthesized and characterized by ^{1}H NMR, electronic absorption spectroscopy, and mass spectrometry. The effect of the nature of functional groups within iron complexes on the redox processes involving these complexes in water–alkaline solutions is analyzed. Electronic transitions in the ligand ($E_{red/ox}$ = 0.820–0.850 V) and the metal ($E_{red/ox}$ = −0.005 to −0.190 and −0.790 to −0.870 V for the $Fe^{4+} \leftrightarrow Fe^{3+}$ and $Fe^{3+} \leftrightarrow Fe^{2+}$ transitions, respectively) were found in the cyclic voltammograms. Iron in the synthesized complexes **I**–**IV** under the conditions under study exists in the +4 oxidation state. The activity of iron complexes in electroreduction of molecular oxygen significantly depends on the nature of a substituent, increases in the series: Fe(*ms*-*p*-NO_2Ph)$_3$Cor (**II**) < Fe(*ms*-*p*-MeOPh)$_3$Cor (**I**) < Fe(β-Br)$_8$(*ms*-Ph)$_3$Cor (**IV**) < Fe(*ms*-Ph)$_3$Cor (**II**) and is caused by the fact that low-energy redox electron transitions occur in the molecules. The electrocatalytic activity of iron corroles is much higher than that of metal porphyrins with a similar structure.

DOI: 10.1134/S0036023617120051

The interest in investigation of porphyrin (H_2P) analogues with the modified structure of the coordination center N_xH_y, such as corroles, is due to their potential use as catalysts and electrocatalysts, photosensitizers, and other components of hybrid nanomaterials for various applications [1–8]. Development of electrocatalysts for reduction of molecular oxygen and chemical current sources based on these electrocatalysts is a relevant field of application of metal corroles [1, 9].

Compared to porphyrins, corroles have a number of important features in their geometrical and π-electron structure. Hence, these trianionic ligands can stabilize metals in higher oxidation states (e.g., Mn^{4+}, Fe^{4+}, Ni^{3+}, Cu^{3+}, Ag^{3+}, etc.) that are not typical of porphyrin–metal complexes (MP) within metal corroles (MCor). The reason for this stabilization is that metal corroles exhibit non-innocent behavior and redox activity of ligands [1, 10, 11], which consists in possibility of intramolecular electron transitions M ⇆ L in these compounds. These properties draw a significant interest to them as objects of electrochemical research [9–13]. Almost all measurements conducted earlier were performed in organic solvents.

Electroreduction of oxygen in aqueous solutions is a complex reaction running via two main pathways. The first one consists in two-electron transfer giving rise to hydrogen peroxide or a peroxide ion in the acidic or alkaline medium, respectively. The second pathway involves four-electron transfer yielding water or hydroxide ion in the acidic or alkaline medium, respectively (1), (2) [9].

$$O_2 + 2\bar{e} + H_2O \rightleftarrows HO_2^- + OH^-, \quad (1)$$

$$O_2 + 4\bar{e} + 4H_2O \rightleftarrows 4OH^-. \quad (2)$$

The dissociation energy of the O–O bond (494.04 kJ/mol) is relatively high. Most electrode materials facilitate two-electron reduction that releases approximately half of the free energy compared to the free energy of the four-electron reduction reaction. Hence, in order to obtain the maximum free energy during cathodic reduction, one needs to make the reaction run via the four-electron pathway. One of the methods is to use metal complexes with aromatic macroheterocycles for this purpose; however, the result will depend on ligand structure and metal nature in this case [9].

This work continues the previous studies focused on the effect of chemical modification on the electrochemical behavior of metal-*meso*-triphenylcorroles: metal nature (M(*ms*-Ph)$_3$Cor, M = Cu, Zn, Co, Mn) [14], complete

β-octabromo substitution (M(β-Br)$_8$(*ms*-Ph)$_3$Cor, M = Cu, Co, Mn, Fe) [1], *para*-substitution of the phenyl rings of macrocycles using the copper and manganese complexes as an example [15]. The electrochemical characteristics of iron *meso*-triphenylcorroles Fe(*ms*-4-MeOPh)$_3$Cor (**I**) and Fe(*ms*-4-NO$_2$Ph)$_3$Cor (**II**) were also studied previously. The effect of substituents on the shape of cyclic voltammograms (CV) and activity of compounds in electroreduction of oxygen at the electrode–electrolyte solution interface were investigated.

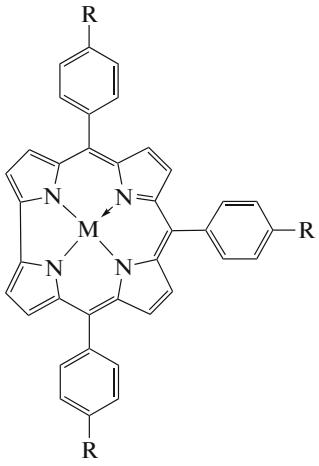

I. M = Fe, R = OCH_3
II. M = Fe, R = NO_2

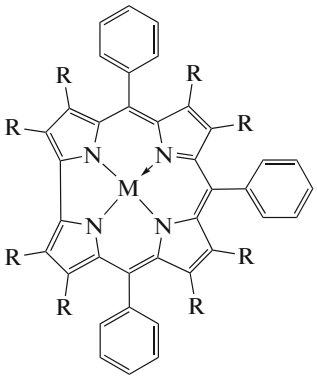

III. M = Fe, R = H
IV. M = Fe, R = Br

EXPERIMENTAL

meso-Phenyl-substituted corroles **I** and **II** were synthesized and purified using the procedures described in [16, 17].

Complexes **I** and **II** were synthesized using the following procedure: a solution of 0.95×10^{-4} mole of iron(II) chloride tetrahydride in DMF was added to the solution containing 0.95×10^{-5} mole of corresponding corrole in 10 mL of DMF. The reaction mixture was brought to boil for 15 min; the complex was then isolated by diluting the reaction mixture with water and extracting metal corrole with chloroform followed by distilling off the solvent. The product was purified by silica gel column chromatography (chloroform was used as an eluent). The yield of the products was ~60%.

The purity and individuality of the products was controlled by thin-layer chromatography (Silufol C60, $CHCl_3$ used as an eluent), electronic absorption spectroscopy (Shimadzu 2000), ^{1}H NMR spectroscopy (Bruker Avance 500), and MALDI-TOF mass spectrometry (Shimadzu Biotech Axima Confidence).

Fe(*ms*-4-MeOPh)$_3$Cor (**I**): [λ (nm), (logε), $CHCl_3$]: 382 (4.26), 416 (4.21), 517 (3.92), 640 (3.64) (sh), [λ (nm), DMF]: 382, 417, 518, 570 (sh); ^{1}H NMR ($CDCl_3$): paramagnetic complex in the range from –42.9 ppm (*meso*-phenyl protons) to +26.8 ppm (β-CH-protons); MALDI FAB MS: M^+ = 669.43 at a calculated FW = 669.55.

Fe(*ms*-4-NO$_2$Ph)$_3$Cor (**II**): [λ (nm), (logε), $CHCl_3$]: 421 (5.00), 513 (4.18), 550 (4.02), 589 (3.92), 643 (3.81), [λ (nm), DMF]: 418, 512, 550 (sh), 645; ^{1}H NMR ($CDCl_3$): paramagnetic complex in the range from–42.3 ppm (*meso*-phenyl protons) to +33.9 ppm (β-CH-protons); MALDI FAB MS: M^+ = 714.80 at a calculated FW = 714.46.

Electrochemical measurements were carried out by cyclic voltammetry in a three-electrode electrochemical cell (the YaSE-2 model): platinum and silver/silver chloride electrodes were used as a polarizing and a reference electrode, respectively. A carbon graphite rod was used as a working electrode. Active mass prepared in an ethanol solution was applied onto the working surface of the electrode (S = 0.64 cm^2; thickness, 0.2–0.3 mm). The active mass consisted of the carbon support (P-514 industrial grade carbon black; State Standard GOST 7885-86; 0.45% ash content), fluoropolymer suspension (6% FP-4D), and a catalyst sample at a 7 : 2 : 1 weight ratio. Final heating of the active mass was conducted at 573 K for 1 min.

Measurements were performed using a P-30J potentiostat/galvanostat system. When studying the redox processes occurring on the surface of the initial electrode and the one modified with corrole samples, argon (99.99%) was bubbled through the electrolyte at a rate of 0.14 mL s^{-1} for 40 min. The working electrode was then immersed in the electrolyte and cyclic voltammograms were recorded in the potential range of 0.5...–1.5 V. Gaseous oxygen was added to the electro-

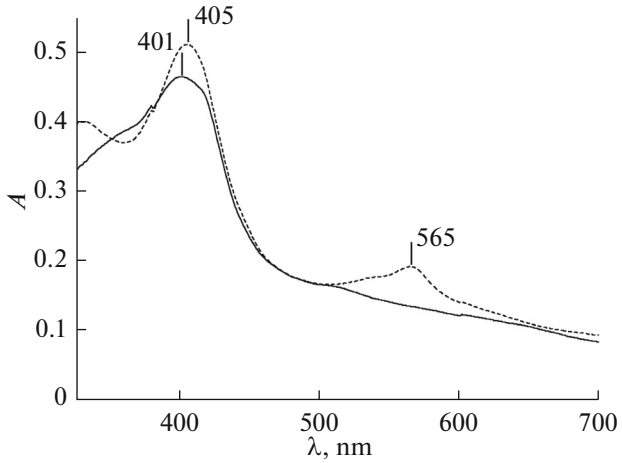

Fig. 1. Electronic absorption spectra of Fe(*ms*-Ph)$_3$Cor (**III**) in $CHCl_3$ (solid curve) and DMSO (dashed curve).

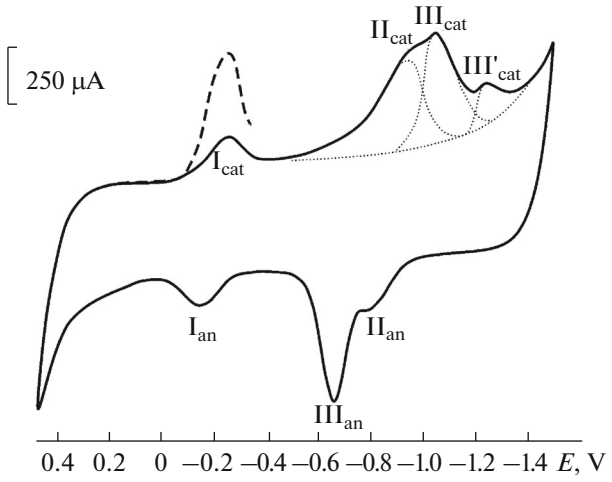

Fig. 2. Voltammogram for the electrode modified with Fe(*ms*-4-MeOPh)$_3$Cor (**I**). Argon (solid curve), saturation with O_2 (dashed curve). 0.1 M KOH; $v = 0.02$ V s^{-1}.

lyte after the measurements in argon atmosphere had been completed. The potentials of the cathodic (E_{cat}) and anodic (E_{an}) maxima for the electrode process involving the compounds under study were detected with an accuracy of ±0.005 V using computer data processing.

RESULTS AND DISCUSSION

Complexes **I** and **II** were prepared by complexation between the corresponding ligand and a tenfold molar excess of metal acetate in DMF medium followed by extraction of the product with chloroform. The reaction of formation of iron complexes requires boiling the reaction mixture under reflux for 15 min, while such complex as CuCor is formed instantaneously after the solutions of the ligand and salt are mixed [1].

Iron corrole complexes exhibit non-innocent properties due to the intramolecular metal–ligand electron transitions, with the formal oxidation of metal being changed [10]. These changes in oxidative state of the central atom are observed already in the solution the solvent is changed. For example, the complex species with the metal in +3 oxidation state (3) is stabilized in electron-donating media (B = DMF, DMSO, Py). Dissolution of the complex in weakly polar solvents with low coordinating ability, especially in the presence of anions (Cl^-, OAc^-), stabilizes the metal in its +4 oxidation state. Hence, additional coordination of either neutral ligands or anionic species to the metal atom shifts the intramolecular redox equilibrium (3). Unlike manganese–corrole complexes [1], the transition is quick in the case of iron complexes. A certain redox species is detected by spectroscopy, for example, according to the typical electronic absorption spectrum (UV-vis, Fig. 1) [1]. In particular, UV-vis spectra of corrole complexes in their lowest oxidation state are characterized by the absence of pronounced bands at 500–700 nm, while the spectra of iron complexes in the oxidation state 4+ contain bands at 520–580 nm [1] (Fig. 1).

$$(X)M^{(n+1)+}Cor^{-\bullet} + Solv \rightleftarrows (Solv)M^{n+}Cor + X^-, \quad M = Mn, Fe. \qquad (3)$$

An electrochemically induced shift in the equilibrium under study can be observed in cyclic voltammographic curves of iron corroles. Two processes of metal electroreduction ($Fe^{4+} \leftrightarrow Fe^{3+}$ and $Fe^{3+} \leftrightarrow Fe^{2+}$, Table 1, Figs. 2 and 3) and the third process related to insertion of an electron into the π-electron system of the macrocycle ($L \leftrightarrow L^{-1}$) are observed for the electrodes containing Fe(*ms*-4-MeOPh)$_3$Cor (**I**) and Fe(*ms*-4-NO_2Ph)$_3$Cor (**II**) under argon atmosphere. Furthermore, an additional redox equilibrium at –0.640 V related to reduction of the nitro group was also detected for compound **II** [18]. A comparative analysis of the effect of functional groups within iron complexes for compounds **I**–**IV** demonstrated that the observed metal-localized redox transitions for metal corroles belong to the potential regions $E_{red/ox}$ = –0.005...–0.190 V and –0.790...–0.870 V, where the stages of electroreduction $Fe^{4+} \leftrightarrow Fe^{3+}$ and transformation $Fe^{3+} \leftrightarrow Fe^{2+}$, respectively, take place (Table 1).

According to the potentials, iron exists in the complexes in the +4 oxidation state under the conditions under study at the first stage of reduction with respect to metal atom, except for the Fe(β-Br)$_8$(*ms*-Ph)$_3$Cor (**IV**) complex whose redox potential is near-zero. Insertion of electron-donating methoxy groups into the *para*-positions of phenyl rings of Fe(*ms*-Ph)$_3$Cor (**III**) increases the potential of the process $Fe^{4+} \leftrightarrow Fe^{3+}$ by 73 mV, while the electron-drawing *meso*-nitrophenyl and β-octabromosubstituted compounds (**II** and **IV**) reduce it by 53 and 112 mV, respectively.

Table 1. Potentials (V, vs Ag/AgCl) of redox transformations for the electrodes modified with iron corroles ($v = 0.02$ V s^{-1})

Compound	Process I $Fe^{4+} \leftrightarrow Fe^{3+}$			Process II $Fe^{3+} \leftrightarrow Fe^{2+}$			Process III $L \leftrightarrow L^{-\bullet}$		
	$-E_{cat}$	$-E_{an}$	$-E_{red/ox}$	$-E_{cat}$	$-E_{an}$	$-E_{red/ox}$	$-E_{cat}$	$-E_{an}$	$-E_{red/ox}$
H_3(*ms*-Ph)$_3$Cor [14]	–	–	–	–	–	–	1.088	0.606	0.847
Fe(*ms*-Ph)$_3$Cor [1]	0.160	0.075	0.117	0.875	0.785	0.830	1.057	0.605	0.831
Fe(β-Br)$_8$(*ms*-Ph)$_3$Cor [1]	0.008	–0.003	0.005	0.842	0.743	0.793	1.029	0.610	0.820
H_2(*ms*-4-MeOPh)$_3$Cor [15]	–	–	–	–	–	–	1.107	–	–
Fe(*ms*-4-MeOPh)$_3$Cor	0.240	0.130	0.190	0.930	0.810	0.870	1.050	0.650	0.850
							1.250	–	–
H_2(*ms*-4-NO_2Ph)$_3$Cor [15]	–	–	–	–	–	–	0.655*	0.555*	0.605*
							1.127	–	–
Fe(*ms*-4-NO_2Ph)$_3$Cor	0.113	–0.015	0.064	0.920	0.820	0.870	0.690*	0.590*	0.640*
							1.050	0.650	0.850

* The electrode process related to the redox properties of the nitro group.

As a water–alkaline solution is saturated with molecular oxygen, the current in the potential range of –0.1 to –0.4 V in the *I*,*E* curves increases significantly due electroreduction of O_2 on the surface of the electrode modified by catalysts. We used the *I*,*E* curves describing the saturation limit of the electrolyte with oxygen to analyze the electrocatalytic activity of compounds **I–IV** in electroreduction of molecular oxygen (Figs. 2 and 3). The increase in electrocatalytic activity causes a significant depolarization effect manifesting itself as a shift in the wave of electroreduction of molecular oxygen $E_{1/2}(O_2)$ towards positive values [14].

The correlation between current density of electroreduction of oxygen and the potentials of the electron containing carbon material and iron corroles (Fig. 4, curves *1–5*) demonstrates that the potential $E_{1/2}$ of the process under study for system without catalyst is –0.30 V, being equal to –0.12 to –0.17 V for iron complexes. The decrease in overvoltage, the shift in the $E_{1/2}(O_2)$ value, as well as the increased current density on the electrode in the presence of iron complexes indicates that an electrocatalytic process is taking place.

The positive effect of the nature of functional substituents on electrocatalytic activity of the complexes under study increases according to growth of $E_{1/2}(O_2)$ as follows: without catalyst (–0.30 V) < Fe(*ms*-*p*-NO_2Ph)$_3$Cor (–0.17 V) < Fe(*ms*-*p*-CH_3OPh)$_3$Cor (–0.14 V) < Fe(β-Br)$_8$(*ms*-Ph)$_3$Cor (–0.13 V) [1] < Fe(*ms*-Ph)$_3$Cor (–0.12 V) [1].

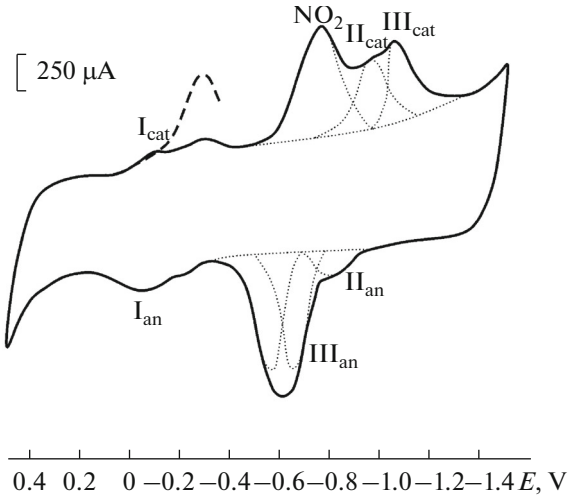

Fig. 3. Voltammogram for the electrode modified with Fe(*ms*-4-NO_2Ph)$_3$Cor (**II**). Argon (solid curve), saturation with O_2 (dashed curve). 0.1 M KOH; $v = 0.02$ V s^{-1}.

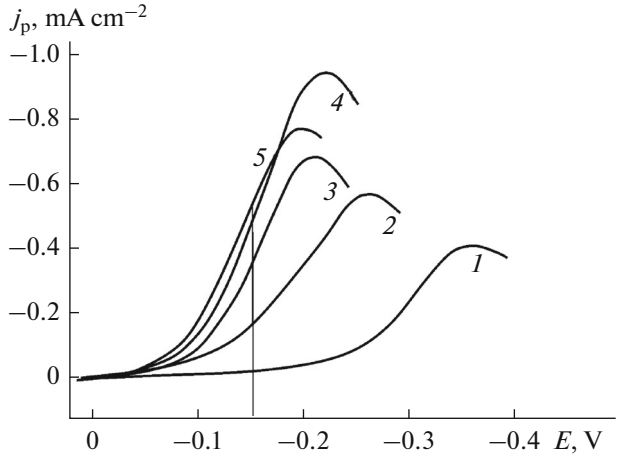

Fig. 4. Current density of electroreduction of molecular oxygen as a function of electrode potentials: (*1*) without catalyst; (*2*) Fe(*ms*-4-NO_2Ph)$_3$Cor (**II**), (*3*) Fe(*ms*-4-MeOPh)$_3$Cor (**I**); (*4*) Fe(β-Br)$_8$(*ms*-Ph)$_3$Cor (**IV**); and (*5*) Fe(*ms*-Ph)$_3$Cor (**III**). Bubbling time, 60 min; $v = 0.02$ V s^{-1}.

Table 2. Parameters of electroreduction of oxygen

Compound	$-E_{1/2}(O_2)$, V	$-j^*$, mA cm^{-2}	n
Fe(*ms*-Ph)$_3$Cor [1]	0.12	0.52	2.5
Fe(β-Br)$_8$(*ms*-Ph)$_3$Cor [1]	0.13	0.47	2.5
Fe(*ms*-4-MeOPh)$_3$Cor	0.14	0.32	2.5
Fe(*ms*-4-NO$_2$Ph)$_3$Cor	0.17	0.14	2.3
without catalyst	0.30	0.03	2.0

* Current density values are given for the electrode potential −0.15 V and the scan rate $v = 0.02$ V s^{-1}.

The findings demonstrate that iron complexes with corrole macrocycles usually provide a more than two-fold decrease in the $E_{1/2}(O_2)$ value compared to the system without a catalyst (−0.30 V). The iron complex with porphyrin, although characterized by the same pattern of substitution as that for compound **III**, has a potential of only −0.25 V [19].

Hence, the electrocatalytic activity of metal corroles is significantly superior to that of metal porphyrins having a similar structure. The electrochemical behavior and electrocatalytic activity of iron–corrole complexes substantially depend on ligand nature; the presence of electron-donating substituents in the macrocycle usually increases electrocatalytic activity [1, 14, 15].

An analysis of the data on potentials for electroreduction of iron corroles ($E_{red/ox}$), which involves a metal and oxygen while being catalyzed by the same metal complex, demonstrates (Tables 1 and 2) that electroreduction in these complexes occurs easier at higher potentials of the equilibrium $Fe^{4+} \leftrightarrow Fe^{3+}$ or, in other words, as stability of the lowest oxidation state of a metal within the metal complex rises.

ACKNOWLEDGMENTS

This work was financial supported by the grant of President of the Russian Federation (number MK-249.2017.3).

REFERENCES

1. N. M. Berezina, V. T. Thao, D. R. Karimov, et al., Russ. J. Gen. Chem. **84**, 737 (2014). doi 10.1134/S1070363214040239
2. J. P. Collman, M. Kaplun, and R. A. Decrreau, Dalton Trans., 554 (2006).
3. L. Simkhovich and Z. Gross, Tetrahedron Lett. **42**, 8089 (2001).
4. J. Grodkowski and P. Neta, J. Phys. Chem. A **106**, 4772 (2002).
5. A. Mahammed and Z. Gross, Angew. Chem. **118**, 6694 (2006).
6. A. N. Biswas, A. Pariyar, S. Bose, et al., Catal. Commun. **11**, 1008 (2010).
7. I. Aviv and Z. Gross, Chem. Commun., 1987 (2007).
8. A. Haber, I. Angel, A. Mahammed, and Z. Gross, J. Diabetes Its Compl. **27**, 316 (2013).
9. S. Huang, Y. Fang, A. Lü, et al., J. Porphyrins Phthalocyanines **16**, 958 (2012).
10. K. P. Butin, E. K. Beloglazkina, and N. V. Zyk, Russ. Chem. Rev. **74**, 531 (2005). doi 10.1070/RC2005v074n06ABEH000977
11. E. Steene, A. Dey, and A. Ghosh, J. Am. Chem. Soc. **125**, 6300 (2003).
12. J. Shen, M. El. Ojaimi, M. Chkounda, et al., Inorg. Chem. **47**, 7717 (2008).
13. A. Schechter, M. Stanevsky, and A. Mahammed, Inorg. Chem. **51**, 22 (2012).
14. M. I. Bazanov, N. M. Berezina, D. R. Karimov, and D. B. Berezin, Russ. J. Electrochem. **48**, 905 (2012).
15. N. M. Berezina, D. R. Karimov, M. I. Bazanov, and D. B. Berezin, Izv. Vyssh. Uchebn. Zaved., Ser. Khim. Khim. Tekhnol. **56** (6), 37 (2013).
16. L. Simkhovich, I. Goldberg, and Z. Gross, Inorg. Chem. **41**, 5433 (2002).
17. R. Paolesse, S. Nardis, F. Sagone, and R. G. Khoury, Org. Chem. **66**, 550 (2001).
18. B. Li, Zh. Ou, D. Meng, et al., J. Inorg. Biochem. **136**, 130 (2014).
19. N. M. Berezina, N. N. Tumanova, Yu. I. Tikhonova, and M. I. Bazanov, Proceedings of the XII International Conference "Synthesis and Applciations of Porphyrins and Their Analogues" (ICPC-12) (Ivanovo, 2016), p. 75 [in Russian].

Translated by D. Terpilovskaya